

Results of the Evaluation and Testing of the Solar Powered AUV and its Subsystems

Mikhail D. Ageev*, D. Richard Blidberg**,
James Jalbert***, Charles J. Melchin**, Donald P. Troop**

*Institute of Marine Technology Problems (IMTP), RAS, FEB, Vladivostok, Russia
Email: ageev@marine.febras.ru

**Autonomous Undersea Systems Institute (AUSI), Lee, New Hampshire
Email: Blidberg@ausi.org; melchin@ausi.org; troop@ausi.org

***Florida Atlantic University, Boca Raton, FL (formerly of AUSI)
Email: jjalbert@bellsouth.net

Abstract:

In July of 1997, a cooperative research program was begun between the Autonomous Undersea Systems Institute and the Institute for Marine Technology Problems (IMTP), Russian Academy of Sciences, Far Eastern Branch, in Vladivostok. In January of 1998, The Office of Naval Research NICOP program funded a joint proposal to evaluate the technologies required for a solar-powered AUV. One of the products of this program was the development, fabrication and testing of a solar AUV engineering prototype (figure 1). The 90 kg. vehicle is 1.7 meters in length, 0.7 meter wide with a pressure case diameter of .24 meters. It has two Solarex (MSX30L) 30 watt solar panels and 32 NiCd cells in a four battery (8 cells in series) configuration. The onboard computer system controls all vehicle functions and records engineering data. This prototype system has undergone at sea testing near Vladivostok, Russia. 48 runs were executed during 22 working days with the objective of defining performance of the vehicle and verifying it's ability to function as a moving platform for long endurance measurements in the ocean. The calculated motion characteristics of the vehicle were compared with calculated ones. Also the properties of vehicle behavior in conditions unique to the SAUV such as sea keeping during drifting or moving on the surface were considered. On the whole, the test results are very positive. These test results will be discussed.

A second vehicle was fabricated at AUSI. This platform is a near duplicate of the IMTP vehicle but contains only a solar energy system. This testbed has been used for at sea testing to determine the effect of wave action on the amount of solar energy collected by the vehicle during recharging. This energy system has

been in continual use at AUSI for 9 months without failure. An energy system testbed (EST) which duplicates the onboard energy system of the SAUV has been fabricated at AUSI in order to investigate alternative energy management strategies. Its solar arrays routinely charge the duplicate battery storage system. System electronics then discharge the batteries during evening hours or when solar energy is not available. The results of these and other similar experiments as well as the at-sea testing accomplished to date have begun to validate initial beliefs of the inherent reliability of this autonomous system. Testing continues to further verify system reliability. The testing of the solar-powered AUV developed in these programs, as well as the development tools such as the energy systems testbed, will be discussed in this paper.



Figure 1 SAUV Engineering Prototype

Sea Test Results:

Sea tests of the SAUV were broken down into three distinct concerns: the effects of biofouling on the power output of the solar panels, measurements of the changes in solar energy acquisition due to sea wave action, and the hydrodynamic characteristics of the prototype SAUV, especially performance in rough sea during running and

drifting.

Biofouling:

Two commercially available solar array panels were used in these experiments - one a “standard”

Solar Panel Worst Case - Biofoul Results

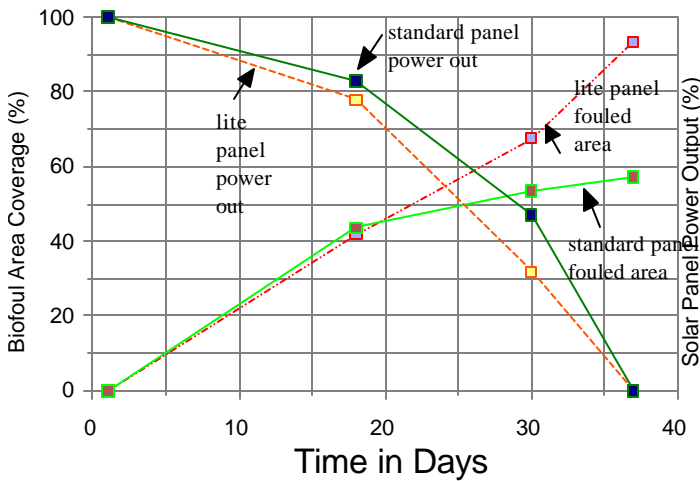


Figure 2: Solar Panel Bio-fouled Area and Power Output versus Time

construction with a tempered glass outer layer, the other a “lite” construction using a Polyvinyl Fluoride outer layer. The solar arrays were submerged about 1 foot below the sea surface at low tide such that they were exposed to the sun all day. After the first 18 days the biofoul cover area was about 42% for both panels and the power output for both panels had reduced to about 80% of maximum. After 30 days the “standard” panel was 53% fouled and had an output power of 47% of maximum while the “lite” panel was biofoul covered 67% and had its output reduced to 32% of maximum. Figure 2 is a plot of solar panel area fouling and output power for both panels. It is apparent that the “standard” panel is more resistant to biofouling and produces more output power after 18 days. Before 18 days the performance is similar. It can be assumed that a solar panel mounted on an SAUV will take longer to biofoul because of the constant washing action over its surface and the fact that the SAUV will take regular excursions into deeper water.

Sea Wave Experiments:

These experiments were designed to measure any decrease in solar energy acquisition either due to sea water washing over the solar panels, or wave motion effects on the solar array angle in varying sea states. An SAUV body having the same surface motion characteristics as the prototype SAUV was designed and fabricated to house the at-sea test system. The system included a Solarex MSX30L solar array, a microprocessor, a battery gas gauge and charge controller (bq2112), and a NiCad battery stack. The system was deployed approximately 3 miles offshore near Portsmouth, NH, USA. Data was taken at sea states 1, 2 and 3. A duplicate system was housed in a land station which also monitored weather data. The two systems were run simultaneously. Figure 3 shows a graph of the percentage difference between the energy acquired by the sea system and the land system.

A positive value in the Y axis indicates that the sea system acquired more energy than the land system while a negative value indicates the opposite. There are two curves in this plot. The top curve represents the actual raw energy acquired while the lower curve indicates the energy with a temperature correction. The correction takes into account three different effects of temperature on charge acquisition: (1) gas gauge compensation factor, (2) battery self discharge compensation factor and (3) solar array temperature effects. The first two factors are utilized by the gas gauge in determining charge actually acquired. As the temperature in the pressure tube increases the energy derating factor increases. Similarly, the temperature of the solar array cells significantly affects the output of

Sea State vs Acquired Solar Energy
Wave Interaction Experiment

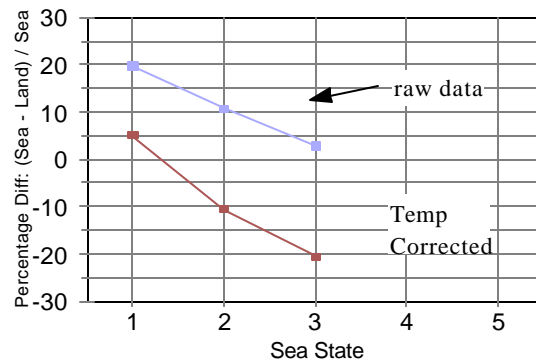


Figure 3: Solar AUV Wave & Water Interaction Data

the solar panels (0.5% per degree C). There was typically about a 10 degree C difference between the environment in the pressure tube at sea (cooler) and on land since the water temperature was typically about 15 degrees C while the air temperature varied from about 20 to 30 degrees C. The temperature difference between the at-sea solar cells and the land solar cells varied between 20 and 35 degrees C. Without temperature correction, the at-sea system appears to have collected more energy than the land based system (at least up to sea state 3). The temperature corrected data indicates that the at-sea system collects slightly more energy up to sea state 1, however, as the sea state increases, the at-sea system acquires less energy and collects about 30% less than the land system at sea state 3. The results of these tests can be incorporated into models of the solar energy system used for predicting energy acquisition under varying sea state conditions.

Hydrodynamic Characteristics: (motion performance characteristics of the vehicle, the drag resistance, characteristics of propulsion system)

The following objectives were pursued during the at-sea testing of the prototype SAUV: 1. functional check, debugging and operational development of the vehicle devices and systems; 2. estimation of the hydrodynamic characteristics and their comparison with calculated data; 3. estimation of the vehicle behavior at rough sea during running and drifting, particularly, flooding of the upper surface of the vehicle and the effect of flooding on operation of the solar cell panels, GPS and radio sets. Tests were conducted in the period between August 18 to October 26, 1998 in depths of 10-30 m. 22 trips and 48 launches of the SAUV were made.

When designing the vehicle, the drag coefficient was estimated to be 0.05-0.07. Characteristic features of the vehicle configuration hinder an exact calculation of the resistance. The actual measured drag coefficient of the finished prototype was much greater ($C = 0.15 - 0.17$). The difference may be due to roughness of the hull surface, additional drag from the edges of the solar panels and insufficient rounding of the wing leading edge. These factors should be taken into account in further work that will require overcoming a number of constructive and technological difficulties.

Motion parameters were calculated based on the

measured motor power and efficiencies, drag coefficients, propeller size and RPM. The estimated data is shown in the Table 1.

| v (m/s) | T (N) | RP M | h _{prop} | h _{moto} r | P _{el} (W) | D ₁₀₀ (km) |
|------------|----------|---------|-------------------|------------------------|------------------------|--------------------------|
| 0.4 | 1.14 | 288 | 0.73 | 0.34 | 1.82 | 79.1 |
| 0.6 | 2.38 | 423 | 0.74 | 0.46 | 4.23 | 51.1 |
| 0.8 | 4.24 | 564 | 0.75 | 0.54 | 8.47 | 34.0 |
| 1.0 | 6.62 | 705 | 0.74 | 0.60 | 14.9 | 24.2 |

v-velocity of the vehicle η_{motor} - motor efficiency
 T- thrust η_{prop} - propeller efficiency
 P_{el}- power consumed D₁₀₀- cruising
 range on a 100 Wh energy basis

Table 1. Motion parameters with $c_x = 0.05$

At the real resistance coefficient the propeller turns out to be ineffective, its efficiency reduces from 0.75 to 0.53. It seems to be advantageous to apply a propeller of greater diameter to reduce losses. Table 2 (top) shows results of calculation for the utilized propeller and (bottom) for the propeller with parameters: D=0.175m, P=0.14m, A=0.15. As can be seen from Table 2 replacing the propeller reduces losses by more than 30%. The data in

| v m/s | T N | RPM | h _{prop} | h _{motor} | P _e W | D ₁₀₀ km |
|----------|--------|------|-------------------|--------------------|---------------------|------------------------|
| 0.4 | 3.55 | 420 | 0.53 | 0.53 | 5.04 | 28.6 |
| 0.6 | 7.99 | 630 | 0.53 | 0.64 | 14.2 | 15.2 |
| 0.8 | 14.2 | 840 | 0.53 | 0.70 | 30.8 | 9.4 |
| 1.0 | 22.5 | 1056 | 0.53 | 0.73 | 58.3 | 6.2 |
| 0.4 | 3.55 | 303 | 0.68 | 0.59 | 3.58 | 40.2 |
| 0.6 | 8.03 | 452 | 0.69 | 0.68 | 10.2 | 21.2 |
| 0.8 | 14.2 | 603 | 0.69 | 0.73 | 22.7 | 12.7 |
| 1.0 | 22.4 | 756 | 0.69 | 0.75 | 43.3 | 8.3 |

Table 2. Motion parameters with $c_x = 0.17$
 (propeller diameter - 0.14 m, below - 0.17 m)
 (Other designations as in Table 1)

Table 2 leads to the following conclusions: 1). The current propeller should be replaced with a propeller of greater diameter with a reduced area ratio. 2). The optimal operating range of SAUV velocities is 0.6-0.8 m/s. The vehicle controllability suffers at lower velocities, and the long cruising range decreases considerably at higher velocities. 3). It is desirable to use a motor with the maximum efficiency of 10-20 W at 400-600 rpm.

Motion control in the horizontal plane:

Controlled motion tests in the horizontal plane were performed both on the surface and during diving. The actual controlled motion correlated well with the modeled performance. During initial launches of SAUV a considerable deviation of the magnet compass was observed. As it was revealed the GPS array placed above the compass was responsible for deviation. A standard method for fastening the array to a steel construction includes the use of magnets. Removal of magnets and change of the attachment method allowed to eliminate the compass deviation. On the whole, adjustment of the heading channel did not cause any difficulties and the system functioned safely during subsequent launches.

Motion control in the vertical plane:

The main difficulty in fulfillment of this part of tests was caused by a low velocity of the vehicle (about 0.4 m/s) owing to the high drag resistance. With such a velocity of motion, the presence of redundant buoyancy (11 N), and stability moment (12.6 Nm), considerable angles of flap and attack angles are required for descent. An additional resistance due to this fact causes still greater reduction of velocity at the fixed rotational speed of propeller. Table 3 gives the data for calculation of the SAUV motion parameters at the constant 420 rpm propeller rotation.

| d | v | T | -y | -q | -a |
|----------|----------|----------|-----------|-----------|-----------|
| 4 | 0.37 | 3.3 | 10 | 0 | 10 |
| 8 | 0.35 | 3.5 | 14.3 | 1.6 | 12.7 |
| 12 | 0.33 | 3.6 | 17.8 | 2.9 | 14.9 |
| 16 | 0.32 | 3.7 | 20.8 | 3.6 | 17.2 |
| 20 | 0.31 | 3.7 | 23.5 | 4.1 | 19.3 |
| 24 | 0.30 | 3.8 | 25.8 | 4.3 | 21.5 |
| 30 | 0.28 | 3.9 | 29.0 | 4.4 | 24.6 |

δ , degree - flap angle,
 V, m/s - velocity, T
 T - propeller thrust
 ψ , degree - trim angle,
 θ , degree - trajectory angle
 α , degree - attack angle.

Table 3. Motion Parameters at 420 RPM

It follows from the data given that an increase in the flap angle results in a marked decrease of the speed and rise of the attack angle " whereas the angle of trajectory 2 remains small even at the maximum deflection of the flap. Increasing the vehicle velocity results in much better movement parameters. Table 4 contains the data corresponding to the descent with a trajectory slope angle equal to -45° .

| v,m/s | 0.4 | 0.5 | 0.6 | 0.7 | 0.8 |
|-----------------|------------|------------|------------|------------|------------|
| d, deg. | 29.5 | 17.6 | 11.8 | 8.43 | 6.35 |
| -a, deg. | 14.1 | 8.65 | 5.86 | 4.25 | 3.22 |
| T, N | 12.4 | 13.9 | 16.1 | 18.9 | 22.1 |

Table 4 descent trajectory slope angle equal to -45°

The propeller thrust required for the preset ascent velocity as seen in Table 5 has a negative value at low velocities and is equal to zero near $v = 0.6$ m/s. Thus, the motor may be switched off during ascent. The energy consumed to overcome the buoyancy force during descent is energy gained during ascent of the vehicle.

| v, m/s | 0.4 | 0.5 | 0.6 | 0.7 | 0.8 |
|-----------------|------------|------------|------------|------------|------------|
| -d, deg. | 29.3 | 18.4 | 12.7 | 9.3 | 7.1 |
| a, deg. | 2.71 | 1.65 | 1.11 | 0.81 | 0.62 |
| T, N | -3.8 | -2.0 | 0.34 | 3.13 | 6.4 |

Table 5 ascent trajectory slope angle equal to $+45^\circ$

Table 6 gives a comparison of experimental and calculated data for the processes of descent and ascent at the depth 10 m.

| | Experiment | | Calculation | |
|----------------|-------------------|---------------|--------------------|---------------|
| | descent | ascent | descent | ascent |
| d, deg. | 16.0 | 6.0 | 16.0 | 10.0 |
| v, m/s | 0.023 | 0.175 | 0.025 | 0.27 |
| q, deg | 4.11 | 4.45 | 4.6 | 6.35 |

Table 6. Comparison of calculated vs empirical ascent / descent data

The low speed of the vehicle motion during trial allowed attention to details of descent and ascent. This

enabled us to study these processes more thoroughly and to examine possibilities for reduction of the energy consumption for descent and ascent. In this respect the most interesting is the process of ascending when the accumulated potential energy of positive buoyancy is used. Parameters of the fixed motion during ascent without the use of thruster can be easily calculated from the condition $T=0$. In this case a force of resistance is equal to the projection of buoyancy force on the direction of movement trajectory. At the small angles of trajectory inclination the value $P \cdot \sin^2$ is small and gliding proves to be impossible. The minimum angle for the prototype SAUV in which gliding is feasible is $2=12^\circ$. Table 7 illustrates the calculated data for the ascent process at different trajectory angles. Due to variation of the values of buoyancy force projections, the attack angle changes radically at $2=33.5^\circ$, when this angle changes sign. In this case the transverse projection is entirely compensated by the lifting force of the flap.

| q, deg. | v, m/s | -d, deg. | a, deg. |
|----------------|---------------|-----------------|----------------|
| 12 | 0.30 | 4.4 | -12.6 |
| 15 | 0.35 | 10.3 | -7.2 |
| 30 | 0.49 | 13.7 | -0.7 |
| 33.5 | 0.52 | 13.5 | 0 |
| 45 | 0.59 | 13.2 | 1.2 |
| 60 | 0.65 | 12.9 | 2.2 |
| 75 | 0.68 | 12.5 | 2.9 |
| 90 | 0.7 | 12.1 | 3.5 |

Table 7 Ascent at various angles

Because gliding is possible only at $2 > 12^\circ$ the vehicle is incapable of beginning an ascent without the aid of the thruster to bring up the motion parameters to the values corresponding to the data of Table 7. Without fulfillment of this requirement the ascent will proceed almost without a change of the pitch angle at very slow vertical velocity and more or less accidental lateral motions. This was shown experimentally during sea trials. A fishing line was fastened to the center of the vehicle bottom and passed through the eye of a ballast weight lying on the sea bottom. The vehicle was pulled to the bottom by hand with the fishing line, then the line was released, beginning the free ascent. The motion was estimated visually, its character resembling the uncontrolled and erratic falling of a leaf.

In many cases it is desirable to provide a free and

controllable ascent of the vehicle due to the buoyancy from the motionless state. To accomplish this the form of the vehicle hull must be such that the point of application of the hydrodynamic force will be substantially shifted to the stern from the center of buoyancy in order to ensure formation of the proper pitch moment. This condition is not fulfilled with the current hull shape.

There is another possibility as well – to replace motion control by means of the flap for the control using the gravity force displacement along the longitudinal direction. This is attractive because removal of the flap will somewhat reduce the resistance and, in addition, a mechanism of the load motion can be located inside the pressure housing under the favorable conditions. In contrast to the flap such device will create only the moment relative to the horizontal transverse axis. A value of this moment can be easily estimated. If a load of the weight W will shift along the longitudinal axis on the value x from the neutral position the load moment at the pitch R will be equal to $M_w = -W \cdot x \cdot \cos R$. Use of the additional load will lead to an increase in weight of the vehicle that is undesirable. In this sense it seems reasonable to use for instance the storage battery. This method has been recently adapted in the prototype SAUV. A storage battery 14 kg in weight moves inside the pressure housing for 0.11m from its middle position. See Figure 4.

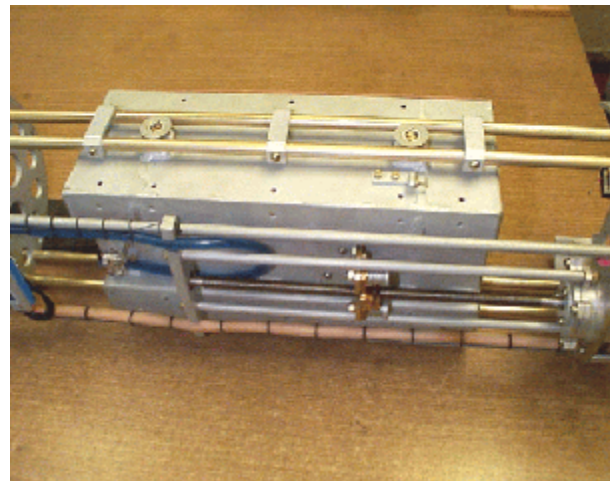


Figure 4: Storage battery as a mechanism of gravity force displacement

Dynamics of the weight control will little differ from dynamics of the flap control if velocities for the change of moment are similar. The recovery from the motionless state turns out to be possible owing to the pitching moment which is formed independently of the

SAUV motion velocity. The load shifts at the preset velocity w up to the final position x_m . The vehicle gains speed v and acquires the pitch R . The ascent mode is established at the time of the order 20 s. Jump of the trajectory angle 2 is due to the fact that its value is determined as a ratio of vertical speed to horizontal one whereas a rise of the horizontal velocity happens later on. Parameters of the stationary processes of descent and ascent at the angles of trajectory 45° are given in Tables 8 and 9 analogous to Tables 4 and 5.

| v, m/s | 0.4 | 0.5 | 0.6 | 0.7 | 0.8 |
|----------------|-------------|-------------|-------------|-------------|-------------|
| x, m | .107 | .103 | .101 | .100 | .099 |
| a, deg. | -5.6 | -3.6 | -2.5 | -1.8 | -1.4 |
| T, N | 11.4 | 13.3 | 15.7 | 18.6 | 21.9 |

Table 8 Descent

| v, m/s | 0.4 | 0.5 | 0.6 | 0.7 | 0.8 |
|-----------------|-------------|-------------|-------------|-------------|-------------|
| -x, m | .098 | .102 | .104 | .105 | .106 |
| -a, deg. | 5.6 | 3.6 | 2.5 | 1.8 | 1.4 |
| T, N | -4.1 | -2.2 | 0.17 | 3.0 | 6.3 |

Table 9 Ascent

Comparison of the data of tables 4, 5 and 8, 9 shows there is less energy consumption in pitch moment control because of the absence of the flap resistance. However, the difference is small. Table 10 shows parameters of free ascent with a change of pitch moment. One drawback of pitch moment control is that a maximum trajectory angle is limited to 50° by the prototype SAUV hull dimensions.

| x, m | v, m/s | q, deg. |
|-------------|---------------|----------------|
| 0.02 | 0.37 | 17.2 |
| 0.04 | 0.46 | 25.9 |
| 0.06 | 0.53 | 34.8 |
| 0.08 | 0.58 | 42.5 |
| 0.10 | 0.61 | 48.9 |

Table 10 Free Ascent

SAUV behavior on the surface:

(Operation of energy system and GPS)

Recharging of the system batteries requires that the vehicle must be on the surface in the daytime hours. During this period the vehicle may drift or move according to the preset program. The working functions of the vehicle include first of all charging of batteries, GPS positioning and communication with the user over radio channel. During this time it is possible to make measurements of various hydrometeorological parameters, for instance, the temperatures of air and superficial layers of water, solar radiation and many other values. In all these cases and also for estimation of the vehicle survivability it is necessary to know the SAUV sea-keeping properties.

The small physical size of the prototype SAUV as compared to sea waves makes it likely that in the rough sea the vehicle may be overturned. That is why it must possess an absolute stability - that is the vehicle must revert to the initial upright position. This is allowed by the vehicle construction and was confirmed in sea tests. The specific form of the vehicle having a wing with the solar panels provides an intensive damping of the roll. Owing to small dimensions and high frequency of free oscillations the vehicle practically follows the wave slope. Measurements of vehicle oscillations on the wave were made together with the other measurements at sea state up to 2-3. Since the waves themselves were not measured the records give only qualitative estimate of the vehicle wave induced oscillations. Taking into account also a visual estimation it can be confirmed that the vehicle tracks an angle of the wave slope. When drifting the vehicle affected by rough sea is oriented by longitudinal axis mainly across the wave crests both toward and along the wave.

An unexpected effect appeared in the form of peculiar accumulation of water in the middle of the deck and formation of the vertical surge. Indeed this is rather simply explained, for instance, if a disk floating on the surface is quickly pushed down then currents of liquid on its surface will be directed to the center where a vertical splash is formed. Since a deck of SAUV does not protrude above the surface a heaving motion of the vehicle leads to arising of such phenomenon. The effect indicated does not influence strongly on the reception of energy by solar panels. The measured performance

correlated well with the rough sea tests of energy collection performed by AUSI.

The operation of satellite navigation and GPS systems was also inspected at sea-tests. A flat antennae was placed into a hermetic hull with a cap of plexiglass. The array was installed in the bow of the vehicle at a height of 3-5 cm from the water surface. During rough sea the flooding of the array body takes place episodically. The function of the GPS was observed at sea states 2 to 3. The unit accurately reported positional coordinates at all times. Also, the time to respond upon power up was checked. In calm seas the time from power up to response was 40 to 70 s and 150 to 190 s in rough seas. Though these results seem acceptable, it may be desirable to increase the antenna height to decrease response time.

Conclusions of sea testing:

- 1). The sea-keeping properties of the prototype-vehicle correspond to estimations adopted during development and satisfy all the requirements of operation.
- 2). The reception of solar energy under conditions of rolling and flooding is satisfactory, the reduction of efficiency caused by incidences of the vehicle hull and panel flooding is partially compensated at the cost of their cooling.
- 3). The GPS navigation system functions safely at the sea state up to 2-3 though the time of its going after switch into the operational mode increases up to 150-190 s.

Energy Systems Testbed:

In order to better understand the technologies involved with the efficient conversion of solar energy, a developmental tool, the Energy Systems Testbed (EST) was designed and built at AUSI. The EST allows the evaluation of different charge algorithms and charging techniques, as well as the integration of differing hardware schemes. Currently, the EST is comprised of a microprocessor with charge algorithm software, two Solarex MSX30L solar arrays, three Sanyo KR-10000M NiCad battery packs, each consisting of eight Nickel Cadmium cells in series, an electronic gas gauge and charge controller (Benchmark bq2112) for each battery pack and various switchable "dummy" loads.[1] The microprocessor is given information about the state of charge of each battery pack from the bq2112, and determines in which mode, charge or run, each pack should be. The controller connects the proper batteries by way of MOSFET switches to either the load or the solar

panel, depending on state.

Preliminary testing of the EST has included comparisons of direct connection of the solar panels to the battery packs with the use of a DC to DC converter between the panel and the battery. The open circuit voltage of the solar panels is about 18V. The fully charged battery is about 12V. Connecting the 18V panel to a 12V battery forces the panel to operate in the constant current mode and may result in less than optimal energy transfer. Placing the DC to DC converter between the panel and battery allows the panel to operate near its open circuit voltage, with the DC to DC converter supplying the charging current to the battery. Preliminary testing on the EST however, has shown no improvement in charge time or efficiency with a simple DC to DC converter implementation. Future experiments will include the implementation of a maximum power point tracker (MPPT) along with the DC to DC converter. The MPPT controls the operating point of the panel at the "knee" between the constant voltage region and the constant current region. It is in this region, where current and voltage are both near optimum, that the panel is supplying the most power possible. MPPT charging has been implemented with some success in the prototype SAUV during at-sea testing, but varying sea and sun states make the data invalid for comparison with other methods. Controlled experimentation on the EST is needed before any conclusions about the benefits of MPPT pertaining to the SAUV can be made.

Most of the work on the EST has involved the development of the charge/discharge algorithm software[6]. NiCad batteries should normally be charged to 80% capacity and allowed to discharge to 20% capacity. Occasionally, a complete charge and discharge cycle, 100% to 0%, must be done to eliminate the "memory effect" associated with NiCad battery chemistry which decreases the battery capacity over time. The current algorithm employed by the EST allows 64 normal charge/discharge cycles before initiating a complete charge/discharge cycle. Charging and discharging between 20 and 80% is called the "Normal" mode. The full charge/discharge cycle is referred to as the "Charge Inaccurate" or CI mode. Figure 5 shows a graph of the charging profile of the three batteries over time, with one battery entering the CI mode while the other two remain in Normal mode. The battery in CI mode begins to discharge as it is switched to the load after hitting 100%. The solar panel is switched to the second battery, in normal mode, which charges to 80%. The battery remains at 80% since

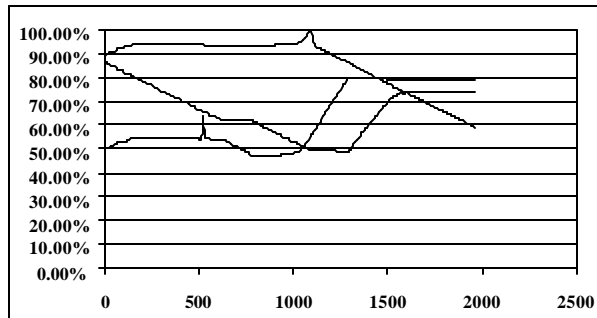


Figure 5. EST Battery Charge/Discharge Profile

no load is attached. The solar panel is then switched to the third battery, also in normal mode, which begins to charge towards 80%. However, night fall occurs when the third battery is at about 75% capacity, the solar panel stops providing energy and charging stops. The battery in CI mode continues to provide power to the load as it discharges towards 0%.

Current Development Objective - a 30 day, at sea, deployment:

The goal of the work being undertaken at AUSI and IMTP is to investigate the potential of Solar Powered AUV (SAUV) in undertaking long endurance, autonomous sampling of the ocean. Although much was accomplished during the initial investigations, theoretical analysis must be verified with empirical data. There is a great deal to be learned from testing that exercises the SAUV for extended periods of time; days, weeks, months. It is only with actual long endurance, in-water testing that we can understand limitations of the subsystems and the long term effect of the ocean environment on the SAUV system. An effort is currently underway that will result in deploying the SAUV system for a 30 day time period. While deployed, the SAUV will be able to communicate with a remote user via an onboard satellite communications system. Test sites will be set up where the AUV can traverse a defined area gathering data during night-time hours. At dawn the AUV will surface to recharge for the day and during that period, transmit its data to a remote shore station via its onboard communications system. The received data will be analyzed by a user and new or modified instructions transmitted to the AUV. At the end of the recharge period it will continue its sampling mission. This process will continue for a period of thirty days and, along with the scientific data, various engineering data will be collected (e.g. available solar energy each day, weather conditions, sea state conditions, engineering data related to the AUV,

The program is a collaborative effort between IMTP, Via Sat Inc, and AUSI. ViaSat has spent 8 years studying oceanographic telemetry and is currently developing the ODL (Ocean Data Link) for satellite communications using geo-synchronous satellites. This new satellite communications link will be integrated with the SAUV system allowing communications with a remote user. The link will also be integrated with the Odyssey vehicle at Woods Hole Oceanographic Institute. In conjunction with the integration of the ODL with SAUV, the development of a user interface will begin. The interface will allow a user to interact with the SAUV and its subsystems. This interface called ASMAC (Autonomous Systems Monitoring and Control) [5] will, when completed, facilitate high-level vehicle operations and control during initial long endurance tests as well as during the long term data gathering deployments.

Four deployments are being planned 1.) A series of in-water long endurance tests to exercise the SAUV system for longer and longer periods of autonomous operation are underway in Vladivostok, 2.) Deployment of the SAUV system at the "AUV fest" to be held in Mississippi in November 1999, 3.) An optional deployment of the SAUV in Penobscot Bay off the coast of Maine to gather oceanographic data in conjunction with an ongoing program at the University of Maine, and 4.) A deployment off of Hawaii to gather oceanographic data in conjunction with the activities being undertaken at the JGOFS HOT site. For each of these efforts, scenarios will be described, mission algorithms determined to accomplish those scenarios, and power management strategies developed to match the environmental parameters unique to each test area, such as solar insolation and local currents, which affect SAUV performance. The purpose of these deployments will be to develop a real understanding of the potential of the SAUV system.

The ultimate goal of the SAUV program is to demonstrate the ability to remotely control and receive acquired data from an autonomous sampling system with extended endurance (weeks to months), via satellite communications. To accomplish this goal, three major objectives have been defined:

A.) To integrate a satellite communications system with the SAUV system and to interface that system with an Autonomous Systems Monitoring and Control (ASMAC) user interface program to facilitate high-level vehicle operations and control. Once the communications system has been integrated with the Odyssey and SAUV systems,

we will verify the ability to send commands to, and receive data from, an AUV via satellite communications. B.) To verify the feasibility of using a SAUV to autonomously acquire oceanographic data and relay that data to a remote user on a regular basis by conducting a 30 day autonomous data gathering experiment, and to implement operational scenarios and power management strategies to account for the environmental parameters impacting SAUV system performance and determine how closely actual performance matches the calculated performance.

C.) To modify the SAUV system as necessary to undertake the proposed long endurance testing and oceanographic data gathering deployments.

The first year will focus primarily on the integration and testing of the satellite datalink on the SAUV. There are two demonstrations planned during this first year, the first will be to demonstrate the current prototype satellite datalink on the SAUV at the November 1999 AUV fest. The second will demonstrate the improved satellite datalink on the Odyssey AUV and the SAUV (June 2000). All of these efforts logically lead to a 30 day scientific data gathering deployment of the SAUV system.

References:

- [1] Blidberg, D.R., Jalbert, J.C., and Ageev, M.D., 1998: "Experimental Results; The AUSI/IMTP Solar Powered AUV Project", MTS Oceans Community Conference, Baltimore, MD, November 16-19, 1998.
- [2] Blidberg, D.R., Jalbert, J.C., and Ageev, M.D., 1998: "A Solar Powered Autonomous Underwater Vehicle System", International Advanced Robotics Program, (IARP), Feb 17-19, 1998.
- [3] Ageev, M.D., and Blidberg, D.R., 1998: "Current Progress in the Development of a Solar Powered Autonomous Underwater Vehicle (AUV)", UT '98, April 15-17, 1998.
- [4] Ageev, M.D., 1999: "1998 Sea Test Results of the Prototype Solar Powered Autonomous Underwater Vehicle (SAUV)", AUSI Technical Report # 9903-01, March 1999.
- [5] Chappell, S., Komerska, R., Peng, L., 1999: "Cooperative AUV Development Concept (CADCON) - An Environment for High Level Multiple AUV Simulation", 11th International Symposium on Unmanned Untethered Submersible Technology, Durham, NH, August 23 -25, 1999.
- [6] AUSI, "Energy System Testbed Investigation" AUSI Technical Report # 9909-01, in process